IOP Conf. Series: Materials Science and Engineering **450** (2018) 032036 doi:10.1088/1757-899X/450/3/032036

Modeling of electron beam distribution in electron beam welding

Yu N Seregin, A V Murygin, V D Laptenok and V S Tynchenko

Reshetnev Siberian State University of Science and Technology, 31 Krasnoyarsky Rabochy Av., Krasnoyarsk, 660037, Russian Federation

E-mail: vadimond@mail.ru

Abstract. The results of mathematical simulation of the electron beam distribution during heating of AMG-6 alloy by moving instantaneous energy sources equivalent to a beam in electron-beam welding are presented in the article. The calculations were carried out using the functional developed by the authors. The paper presents the results of calculations and an algorithm for searching for the optimal technological regime of electron beam welding, which can be recommended for designing electron-beam welding technology for new construction materials or for upgrading old process technology. The results of modeling the technological process for welding a 2.4-cm thick plate made of AMG-6 material, which were compared with the experimental data obtained under laboratory conditions, are presented in this paper.

1. Introduction

At present, in the production of modern products, there is a need to combine dissimilar materials. The limited availability of information on the connection of dissimilar materials stimulates research in this direction [1]. The use of electron-beam welding for joining various material alloys led to a new wave of research [2-7], according to which the designers select the most suitable parameters of the technological process, with reference to a specific material used in production. Depending on the requirements, various methods of welding are widely used. Among them, electron-beam welding (EBW), in connection with the use of vacuum equipment, is distinguished by the ability to solve most problems in the design and manufacture of structural metallic materials products [8-12].

The main advantages of EBW are provided by achieving high energy density in the electron beam, controllability of its parameters and the possibility of fully automating the welding process. High welding speed, deep and narrow welds and minimum value of the thermal influence zone in electron-beam welding cause its wide application.

The quality of the seam at EBW is determined by the combination of technological and energy parameters of the process. Maintenance of the welding process energy parameters at the required level ensures, under the same technological conditions, the constancy of the welded joint operational parameters, geometric dimensions, structural, strength and other parameters. However, the possibility of forming a unique "dagger" shape with minimal metal capacity of the welding bath comes into conflict with the achievement of stable operating parameters of the welded joint. Violation of the EBW optimal mode often leads to the appearance of defects in the seams, even on well-welded materials [8].

To prevent root defects, it is necessary to form a steam-dynamic channel with a sufficiently wide lower part and a rounded bottom. The shape of the channel is changed with the electron beam power distribution shape in the welding zone. The most effective way to influence the formation of the penetration channel is the electron beam oscillation. When welding metals with a horizontal beam, it is possible to significantly widen the diameter and increase the stability of the channel in the weld pool, which has a positive effect on the stability of seams formation: the spattering of molten metal is reduced, and the melt is prevented from flowing out of the bath.

There are a lot of scientific collectives, which math the processes accompanying the EBW. The ways of finding solutions are very diverse. Some are directed toward modeling the heating source [13], its spatial position relative to the material to be welded [14], models are proposed that predict the geometric characteristics of the weld [15]. Other works [16] offer mathematical models on which it is possible to obtain adequate parameters of the technological process depending on the materials to be connected.

Authors' preliminary research revealed the prospects of new scanning paths in order to improve the technology of electron beam welding to make welded joints of better quality. For this purpose, was developed mathematical models and an algorithm for electron-beam welding optimal technological regime searching, which can be recommended for testing EBW technology of new construction materials or improvement of existing old technical processes.

The algorithm consists of three stages:

1. Choice of the electron beam oscillations trajectory;
2. Correction of the selected electron beam oscillations trajectory shape;
3. Calculation of welding process parameters.

Experimental studies were carried out on an electron-beam installation ELU-5 with electron beam equipment and a CEP-2 gun with a Ø4.7 mm tablet. Welding was performed on annular specimens Ø300 mm with a thickness of 24 mm made of AMg-6 material.

2. Choice of the electron beam oscillations trajectory

Due to the fact that the size of the scanning path always significantly exceeds the diameter of the electron beam itself, it is advisable to represent the electron beam in the form of an energy point source moving along the chosen trajectory at a rate proportional to the frequency of the electron beam oscillation. The method is based on the mathematical model of a moving point source on the surface of a semi-infinite body [8]:

$$T(x,y,z,q,v,t) = T_I + \frac{2q}{c\rho\sqrt{(4\pi a)^3}} e^{-\frac{vx}{2a}} \int_0^t exp\left(-\frac{v^2\tau}{4a} - \frac{R^2}{4a\tau}\right)\frac{d\tau}{\tau^{3/2}}. \quad (1)$$

where T – material temperature [^{0}C], (x, y, z) – coordinates [cm], q – heating source energy [J], v – heating ratio [cm/sec.], t – integration time interval [sec.], T_I – initial temperature of the material [^{0}C], $c\rho$ – bulk heat capacity of the material [J/(cm^{2}K)], a – thermal diffusivity of material [cm^2/sec.], R – radius [cm] ($R=(x^2+y^2+z^2)^{1/2}$), τ – current integration time [sec.].

Most beam scanners contain digital-to-analog converters, so it is easy to convert the scan form of an electron beam in the form of moving it along a grid. For the analysis, the trajectories frequently encountered in production were selected (figure 1).

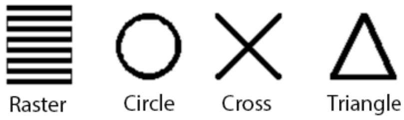

Figure 1. Forms of the investigated electron beam scanning trajectories.

As a measure for the analysis of trajectories, the next functional was chosen:

$$J = \sqrt{\frac{1}{n-1}\sum_{i=1}^{n}\left(T_{Ii}(x,y,z,q,v,t) - \overline{T_I(x,y,z,q,v,t)}\right)^2}; \quad (2)$$

where $T_{Ii}(x,y,z,q,v,t) = \frac{T_i(x,y,z,q,v,t)}{T_{\max}(x,y,z,q,v,t)}$; $T_i(x,y,z,q,v,t)$ – temperature, calculated by (1); $\overline{T_I(x,y,z,q,v,t)}$ – mean temperature; $T_{\max}(x,y,z,q,v,t)$ – maximum temperature.

The criterion for choosing the scanning path is the minimum value of the functional J_{min}. The calculated values of the functional for different scanning trajectories are shown in figure 2.

3. Correction of the selected electron beam oscillations trajectory shape

Having chosen the shape of the electron beam scanning path, it is necessary to evaluate the influence of each segment of this trajectory shape on the functional (2) value. If the plot affects the increase in the functional, then it should be removed from the form, redistributing the energy input of this site to the rest.

After performing these actions, a new shape of the scan path was obtained (figure 3). The calculated functional values as a function of the intervals δ for the selected corrected scan paths are shown in figure 4.

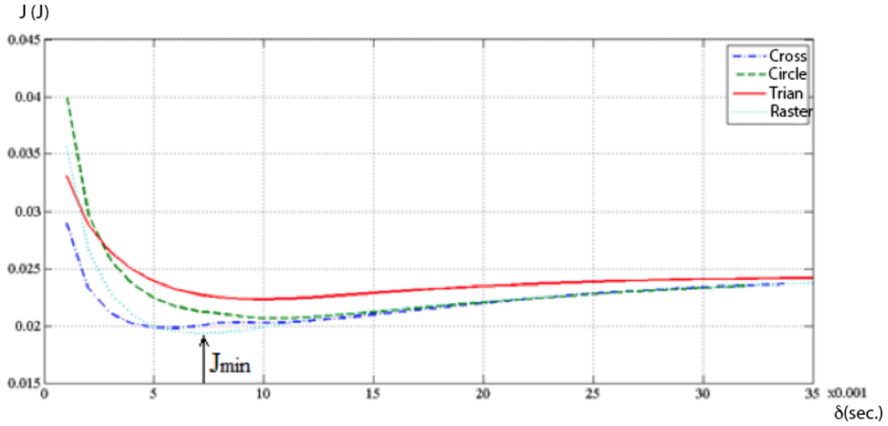

Figure 2. Graphs of the functional change depending on the interval between the positioning points for the investigated electron beam scanning trajectories.

Figure 4 shows that the minimum of the functional is achieved with the scanning path of the electron beam in the form of "Rastr_Optima". Therefore, according to the calculations, this form should have the best quality indicators.

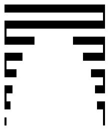

Figure 3. The shape of the electron beam scanning trajectory "Rastr_Optima".

To test the theoretical results, experiments were carried out using scanning trajectories of the electron beam "Rastr" and "Rastr_Optima". Trial experiments on AMG-6 material (figure 5) showed the following results. When scanning an electron beam in the form of "Rastr", the shape of the seam shows "dagger" properties. When scanning an electron beam in the form of "Rastr_Optima", most of the energy of the beam is spent on heating the metal over the entire depth, therefore, "dagger" properties do not appear.

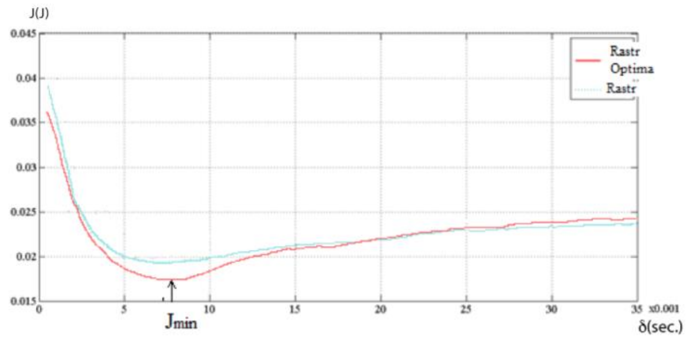

Figure 4. Graphs of the functional change depending on the interval between the positioning points for the investigated electron beam scanning trajectories.

IOP Conf. Series: Materials Science and Engineering **450** (2018) 032036 doi:10.1088/1757-899X/450/3/032036

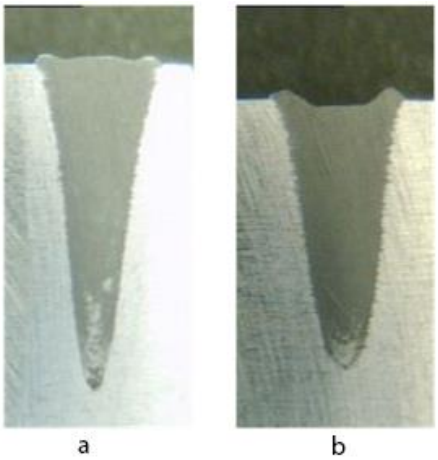

Figure 5. Photomicrographs of AMG-6 samples obtained at EBW scan path (f_{scan}=1000Hz): a) "Rastr"; b) "Rastr_optima".

4. Calculation of welding process parameters

The following welding process parameters were investigated in this work: welding speed and current, amplitude of scanning along the established electron beam trajectory, position of the focal spot relative to the surface of the welded product.

To simulate the electron beam, taking into account the thickness of the welded article, a heating source was considered, representing the following expression:

$$T_i(x, y, z, q, v, t) = T_1(x, y, z, q, v, t) + T_2(x, y, z, q, v, t); \quad (3)$$

where $T_1(x, y, z, q, v, t)$ и $T_2(x, y, z, q, v, t)$ – mathematical models of movable point (1) and linear source (4),

$$T_2(x, y, z, q, v, t) = T_I + \frac{q}{4\pi\lambda\delta} e^{-\frac{vx}{2a}} \int_0^t exp\left(-\frac{v^2\tau}{4a} - \frac{2\lambda\tau}{c\rho\delta} - \frac{(x^2+y^2)}{4a\tau}\right)\frac{d\tau}{\tau}; \quad (4)$$

The combination of sources is caused by the need to take into account the effect on the thermal field of the product thickness. The welding speed is explicitly present in formulas (1) and (4), so it can be found by solving the inverse problem:

$$v = \min_{v_{min} \div v_{\max}} J; \quad (5)$$

To this point, modeling the behavior of the chosen functional with a variation in the welding speed, we determine the solution of the problem at the point where the functional undergoes a minimum.

The welding current is not represented in the formulas of the thermal process, but it is related to the energy of the heating source Q by the following expression:

$$I_{weld} = \frac{Q}{U \cdot \eta \cdot 0{,}24} [mA]; \quad (6)$$

where U – accelerating voltage [kV]; η – efficiency of EBW (usually is about 0,89).

The purposed developed algorithm is based on the following assumption: since the heat welding process is not stationary, it is advisable to select the source energy (or welding current) at which the value of the functional did not change in the event of an increase in the integration time at some limit. For this purpose, a family of curves should be constructed for the dependence of the functional on the integration time for different values of the heating source energy. Then the energy value at which the curve has the smallest slope is selected. When carrying out experimental studies, such welding current was $I = 343\ mA$.

The scanning amplitude of the electron beam is determined at the stage of choosing the geometric parameters of the integration volume for mathematical models (1) and (4). First, the value of the temperature threshold defining the boundaries of the investigated volume of the heated material is calculated:

$$T_{threshold} = \min_{T_{min} \div T_{max}} J. \quad (7)$$

During calculation of the functional (2) dependence on the heating temperature (7), the propagation boundaries of the variable temperature are formed, the intersection points of which with the threshold temperature form the beam scanning amplitudes respectively along and across the welding direction. When carrying out experimental studies, such amplitudes were $x = 0{,}23\ cm$ and и $y = 0{,}22\ cm$ accordingly.

Carrying out the calculations for (5), moving the position of the heating point source along the depth of the heated material, it can be modeled the dependence of the functional on the focal length of the electron beam. As a result, the position of the functional minimum indicates the coordinate of the optimal focal spot position of the electron beam relative to the surface of the welded product.

Similar studies carried out on the VT-14 titanium alloy suggest that the models proposed by the authors and the search algorithm for the optimal technological regime of electron beam welding can be applied to other alloy materials.

5. Conclusion

The proposed mathematical models cover not the entire welding process, but only the phase of metal heating before the phase transition, therefore the optimization criterion is applicable only for the time of welding zone heating. The proposed algorithm can be used for welding with a non-scanning electron beam, but the analysis of the shapes of oscillation trajectories should be excluded. It is advisable to use the results of the work when testing new electron beam scanning paths to reduce the costs of experiments and to evaluate the effectiveness of using a new scanning shape.

Further investigations by the authors in the chosen direction could give positive results not only in the modeling of the electron beam distribution, but also in modeling the power of the heating source in electron-beam welding.

Acknowledgments

The reported study was funded by RFBR and Government of Krasnoyarsk Territory according to the research project № 17-48-240098.

References

[1] Sun Z and Karppi R 1996 The application of electron beam welding for the joining of dissimilar metals *Journal of Materials Processing Technology* **59(3)** 257-67
[2] Yunlian Q, Ju D, Quan H and Liying Z 2000 Electron beam welding, laser beam welding and gas tungsten arc welding of titanium sheet *Materials Science and Engineering* **280(1)** 177-81
[3] Kenyon D M 1965 Electron-beam welding *Electronics & Power* **11(8)** 268-71
[4] Barreda J L, Santamarıa F, Azpiroz X, Irisarri A M and Varona J M 2001 Electron beam welded high thickness Ti6Al4V plates using filler metal of similar and different composition to the base plate *Vacuum* **62(2-3)** 143-50
[5] Olszewska K and Friedel K 2004 Control of the electron beam active zone position in electron beam welding processes *Vacuum* **74(1)** 29-43
[6] Guoqing C, Binggang Z, Wei L and Jicai F 2011 Crack formation and control upon the electron beam welding of TiAl-based alloys *Intermetallics* **19(12)** 1857-63
[7] Chaturvedi M C, Richards N L and Xu Q 1997 Electron beam welding of a Ti–45Al–2Nb–2Mn+ 0.8 vol.% TiB2 XD alloy *Materials Science and Engineering* **239** 605-12
[8] Rykalin N N, Zuev I V and Uglov A A 1978 *Fundamentals of electron beam processing of materials* (Moscow: Mashinostroyeniye)
[9] Shiller Z, Gaizig U and Panzer Z 1980 *Electron beam technology* (Moscow: Energiya)
[10] Nazarenko O K, Kaidalov A A and Kovbasenko S N 1987 *Electron-beam welding* (Kyiv: Naukova dumka)
[11] Orlinov V and Mladenov G 1982 *Electronic and ionic methods of processing and analysis of the*

IOP Conf. Series: Materials Science and Engineering **450** (2018) 032036 doi:10.1088/1757-899X/450/3/032036

substance (Sofia: Technika)
[12] Mladenov G 2009 *Electronic and ionictechnologies* (Sofia: Prof. Marin Drinov)
[13] Rouquette S, Guo J and Le Masson P 2007 Estimation of the parameters of a Gaussian heat source by the Levenberg–Marquardt method: Application to the electron beam welding *International Journal of Thermal Sciences* **46(2)** 128-38
[14] Koleva E 2005 Electron beam weld parameters and thermal efficiency improvement *Vacuum* **77(4)** 413-21
[15] Koleva E 2001 Statistical modelling and computer programs for optimisation of the electron beam welding of stainless steel *Vacuum* **62(2-3)** 151-7
[16] Zäh M F and Lutzmann S 2010 Modelling and simulation of electron beam melting *Production Engineering* **4(1)** 15-23